

A Three-Dimensional Vp Model of the Southeastern Taiwan Area and Its Tectonic Implications

Win-Bin Cheng^{1,3}, Chengsung Wang², Chuen-Tien Shyu³
and Tzay-Chyn Shin¹

(Manuscript received 24 March 1998, in final form 1 September 1998)

ABSTRACT

Using travel time data from local earthquakes and air-gun shots recorded by the Central Weather Bureau Seismographic Network, the transition from a typical subduction to a collision suture in the southeastern Taiwan area is imaged in terms of a three-dimensional Vp structure. The southern prolongation of the Longitudinal Valley Fault (PLVF), which is characterized by a sharp contrast in velocity on either side, is the primary feature in the velocity structure. West of the PLVF, a high velocity volume exists from the surface to about 9-km in depth, which can be interpreted as being related to the Central Range. The Central Range structure seems to end near 22.2° N beneath the Hengchun Peninsula. East of the PLVF, a major high velocity anomaly in the middle- to lower-crust beneath the Southern Longitudinal Trough and Huatung Ridge is observed. According to the velocity structure and the estimated composition, the high velocity body could be the forearc oceanic crust, which might have been torn off and separated from the Philippine Sea plate after the Luzon arc was formed, and has been shortened during the collision of the Eurasian and Philippine Sea plates. The other conspicuous feature of the Vp model is a clearly lateral velocity variation across the Taitung Canyon from the surface to about 25-km in depth, which might be associated with the segmentation of the Luzon arc. Using the three-dimensional Vp model, earthquake events that occurred from 1990 to 1997 were relocated. Most of the relocated hypocenters in the study area tend to lie on the locations where there is a greater gradient in the Vp model.

(Key words: 3-D velocity structure, Seismicity, Tectonic structure)

¹Seismological Observation Center, Central Weather Bureau, 64 Kung-Yuan Road, Taipei, Taiwan, ROC

²Institute of Applied Geophysics, National Taiwan Ocean University, Keelung, Taiwan, ROC

³Institute of Oceanography, National Taiwan University, Taipei, Taiwan, ROC

1. INTRODUCTION

The southeastern Taiwan area is tectonically of interest, because of the process of oblique collision between the Eurasian and Philippine Sea plates taking place there. Due to this oblique collision, the convergence intensity increases from south to north (e.g., Suppe, 1984; Lewis and Hayes, 1989). Meanwhile, the action between the Eurasian and Philippine Sea plates also causes numerous moderate earthquakes (Wu, 1978; Pezzopane and Wesnousky, 1989; Huang, 1997). The successive presence of the subduction complex, forearc basins and volcanic islands from west to east implies the existence of obvious lateral variations in the crustal structure (Figure 1). Thus, it is a suitable region in which to study the crustal evolution for the transition zone from a typical subduction to collision.

Based on a morphological study, Chen and Juang (1986) divided the southeastern offshore area of Taiwan into five physiographic zones: the Hengchun Ridge, the Southern Longitudinal Trough, the Huatung Ridge, the Taitung Trough and the Lanhsu Ridge (Figure 1). The relationship between the submarine morphotectonic features and geological units off southeastern Taiwan has also been discussed in the literature using seismic, magnetic, gravity and topographic data (Lundberg, 1988; Liu *et al.*, 1991; Shyu and Chen, 1991; Huang *et al.*, 1992; Yu and Song, 1994). Despite these studies, many aspects of its velocity structure, seismicity and the southward extension of the Longitudinal Valley Fault are still unclear. Although the three-dimensional V_p models beneath the Taiwan area have been constructed and discussed using natural earthquake data (Roecker *et al.*, 1987; Chen, 1995; Rau and Wu, 1995; Ma *et al.*, 1996), their resolution for the southeastern Taiwan offshore area was limited by a lack of offshore data. A detailed three-dimensional velocity model is useful to improve our understanding of the crustal structure of southeastern Taiwan and associated oblique collision tectonics.

During August and September 1995, the seismic, magnetic and gravity surveys of the TAICRUST program were conducted by the R/V Maurice Ewing (Liu, 1995). The air-gun sources, released by the R/V Maurice Ewing using a 20-airgun array were recorded by the land-based Central Weather Bureau Seismographic Network (CWBSN) and offshore ocean bottom seismometers (OBSs) in the southeastern Taiwan area. Since there is seismicity distributed in both the onshore and offshore area, the aim of this work is to invert the P-wave travel time data from local earthquakes and airgun shots to better understand the crustal structure of the southeastern Taiwan area. Since the air-gun data can improve the resolution of the velocity structure at shallow depths and the earthquakes are well distributed in location and depth, we obtain a detailed three-dimensional V_p model. Furthermore, seismic reflection, seismic refraction, gravity, and magnetic data are available for the study area. A joint interpretation of the marine geophysical data, seismicity and the velocity structure obtained allows us to depict the subsurface structural features, such as the fractures and faults in the offshore area that would be the sites for potential major earthquakes.

2. GEOLOGICAL SETTING AND PREVIOUS WORK

The Longitudinal Valley Fault (Figure 1) is the generally accepted plate boundary between the Eurasian and Philippine Sea plates (Biq, 1972; Chai, 1972; Karig, 1973, Wu and Lu,

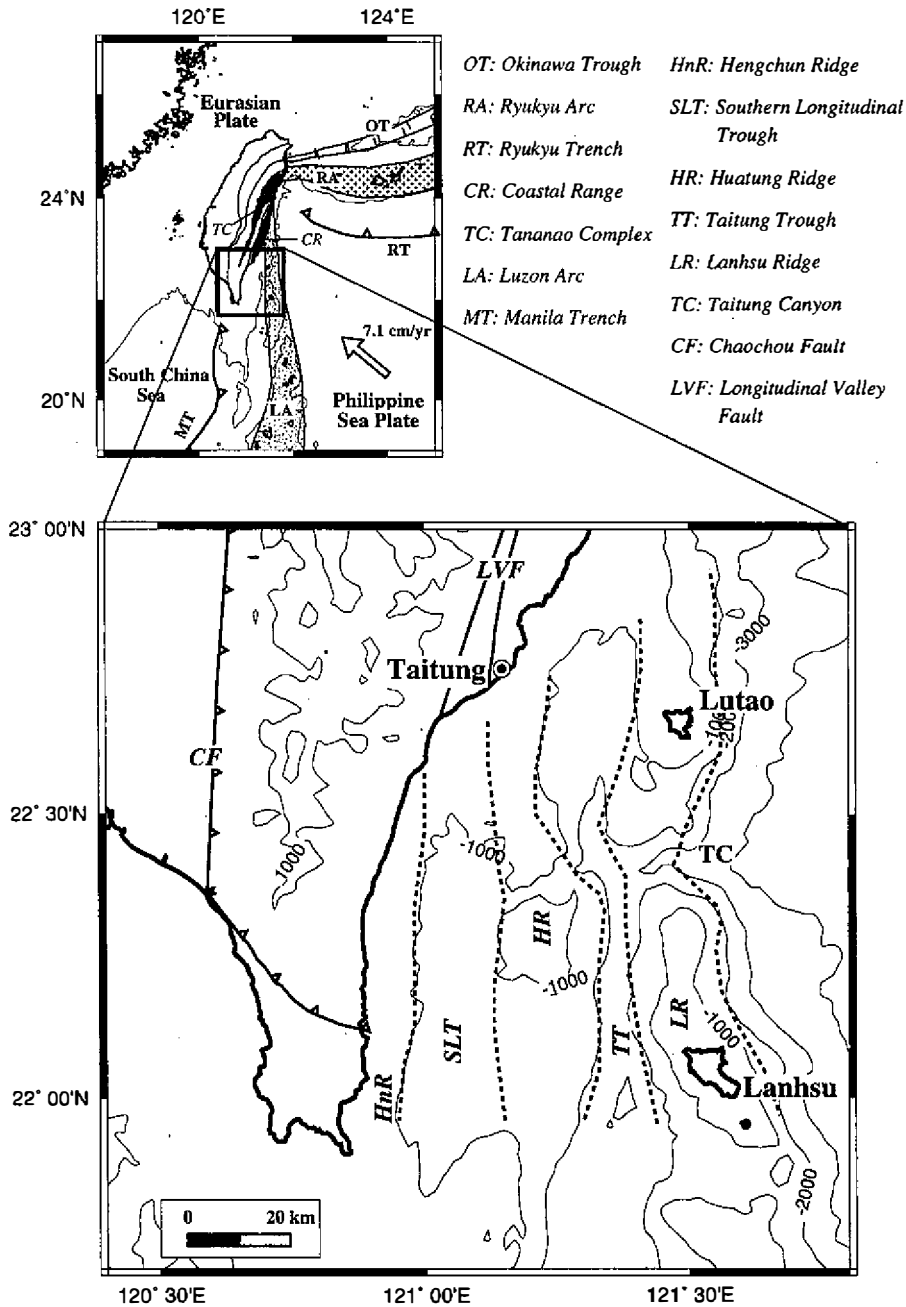


Fig. 1. Location and bathymetry map of southeastern Taiwan. Bathymetry is in kilometers, while offshore dashed lines outline five geological provinces proposed by Chen and Juang (1986). General plate tectonic map of Taiwan is also shown on upper side.

1976; Tsai *et al.*, 1977; Chi *et al.*, 1981; Lin and Tsai, 1981; Hsu and Sibuet, 1995). Based on earthquake data, Lin and Tsai (1981) indicated that the plate boundary extends south-southwest ($N20^{\circ} E$) along the Longitudinal Valley from Hualien to Taitung where it turns southward along the $121^{\circ} E$ meridian just off the eastern coast of the Hengchun peninsula. To the south of the Hengchun peninsula, Hsu and Sibuet (1995) proposed that this boundary turns southwestward and probably connects to the Manila trench.

The Taitung Trough (Figure 1), the northern part of the North Luzon Trough, narrows and shoals toward the north and ends at the southern Coastal Range on eastern Taiwan (Page and Suppe, 1981). Bowin *et al.* (1978) indicated a buried crust to plate boundary along the North Luzon Trough that is filled with thick sediments represented by a sharp gravity low. The tectonic significance of the Taitung Trough is still controversial. Huang *et al.* (1992) consider this trough a forearc basin and not a subduction-related plate boundary.

Lutao and Lanhsu are two northernmost islets of the Lutao-Babuyan ridge of the Luzon arc (Bowin *et al.*, 1978). In the south, the ridge is composed of andesite and some basaltic flows (Ho, 1982). This volcanic belt presumably continues northward, to include the Chimei Igneous Complex in the middle of the Coastal Range of Taiwan (Ho, 1986). Radiometric dating shows a southward younging of volcanic ages in this ridge belt (Richard *et al.*, 1986). In this part of the Luzon arc, the main volcanic activity ceased in the middle Miocene (Ho, 1982, 1986).

The oceanic crust of the South China Sea subducts eastward beneath the Philippine Sea plate along the Manila Trench south of $20^{\circ} N$ (Ludwig *et al.*, 1967; Lin and Tsai, 1981). This convergent tectonics results in a well-defined Wadati-Benioff zone that dips to the east to a depth of more than 200 km (e.g., Roecker *et al.*, 1987; Pezzopane and Wesnousky, 1989). This east-dipping seismic zone extends northward to southeastern Taiwan (to at least $22.5^{\circ} N$) (Wu, 1978; Cardwell *et al.*, 1980; Roecker *et al.*, 1987) but becomes unclear north of $23^{\circ} N$.

From the geophysical and geological studies, five geologic provinces off southeastern Taiwan can be recognized (Chen and Juang, 1986) (Figure 1). Shyu and Chen (1991) noticed that the magnetic basement of the southeastern offshore area of Taiwan can be divided into seven zones which are a result of the recent collision evolution between the Eurasian and Philippine Sea plates. Using magnetic and gravity data, Liu *et al.* (1992) indicated that the material of the basement of the Taitung Trough belongs to a volcanic arc, whereas the basements of the Southern Longitudinal Trough and Huatung Ridge do not. As described by Shyu *et al.* (1996), the northern Luzon arc has changed in direction from NNW-SSE to NNE-SSW at the Taitung Canyon between the Lutao and Lanhsu islets. In the southern offshore area of Taiwan, Fuh *et al.* (1994) reported two sets of strike-slip faults that were induced by forearc block rotation near the Luzon arc and Kaoping canyon.

Apart from a few onshore/offshore seismic refraction studies, (e.g., Cheng *et al.*, 1996a; Chen *et al.*, 1996; Lin *et al.*, 1997a), crustal structure in the southeastern Taiwan offshore area is poorly known. Without offshore data, previous seismic tomographic studies in the study area (Roecker *et al.*, 1987; Ma *et al.*, 1996; Rau and Wu, 1995) have all been rough surveys, and no inversion of earthquake arrival times for the detailed crustal structure has been attempted.

3. SEISMIC DATA AND ANALYSIS

3.1 Travel Time Data

The data set for the inversion should be of high quality and provide best available ray coverage of the region. Two types of travel time data were used in our three-dimensional (3-D) velocity modeling: (1) first-arrival times from airgun shots (Figure 2a) in the southeastern Taiwan offshore area (Cheng *et al.*, 1996b), and (2) first-arrival times of local earthquakes (Figure 2b). Air-gun sources were released by the R/V Maurice Ewing in the southeastern Taiwan offshore area in September 1995. The ray paths of the air-gun shots are dense near the on-land stations, but sparse for the offshore area. The first arrivals of the air-gun shots were quite clear within distances appropriate for modeling as a Pg phase (dashed lines in Figure 3). Arrival times of these air-gun shots provided a strong constraint for the 3-D velocity model, especially at the shallow depths. In addition, the signal recorded by an OBS (Chen *et al.*, 1996) was also included in the 3-D velocity modeling (Figure 2a).

The earthquake data used in this study are P-wave arrival times of local earthquakes recorded by eleven CWBSN stations deployed in southeastern Taiwan (Figure 2b). In this study, we select 595 local earthquakes determined by the CWB that occurred between January 1986 and May 1997, with at least 8 arrival times (both P and S waves) for each earthquake event, a hypocentral depth mostly of less than 50 km, and an RMS error in location of less than 3 km. However, there are also deep events recorded for the study area. These deeper earthquakes tend to be east of the study area and are not as well distributed spatially. Thus only a few of the deeper events are included in the data set. The events used were located within and around the model area and provide spatially distributed ray paths. In particular, the earthquake data recorded at the Lutao station (TWH) during 1986-1991 gave the study area a good coverage of stations. The travel time data were weighted according to their accuracy as inferred from the signal-to-noise ratio of the seismic signals (weightings from 1 to 0.25 for reading errors ranging from 0.01s to 0.1 s for the P wave). The final data set for the inversion consists of 4401 earthquake P-wave arrival times and 641 shot arrival times.

3.2 Method and Inversion Procedure

We applied the 3-D tomographic technique from Thurber (1983, 1993) and Eberhart-Phillips (1990), with documentation by Evans *et al.* (1994), to study the 3-D velocity structure in the southeastern Taiwan area. The velocity of the medium is parameterized by assigning velocity values to the 3-D grid of points. We compiled travel-time data for each receiver as a function of the 3-D spatial location of sources and inverted them for the 3-D velocity structure. Initial hypocenter locations and origin times for earthquakes were input as those determined by the CWBSN. The ray-tracing is done using approximate 3-D algorithm with curved non-planar ray paths (Um and Thurber, 1987). Parameter separation (Pavlis and Booker, 1980) operates on the matrix of hypocentral and velocity partial derivatives so that the hypocentral calculation is separated from the velocity calculation. The damped least-squares approach is used to solve for velocity in the inversion (Thurber, 1983).

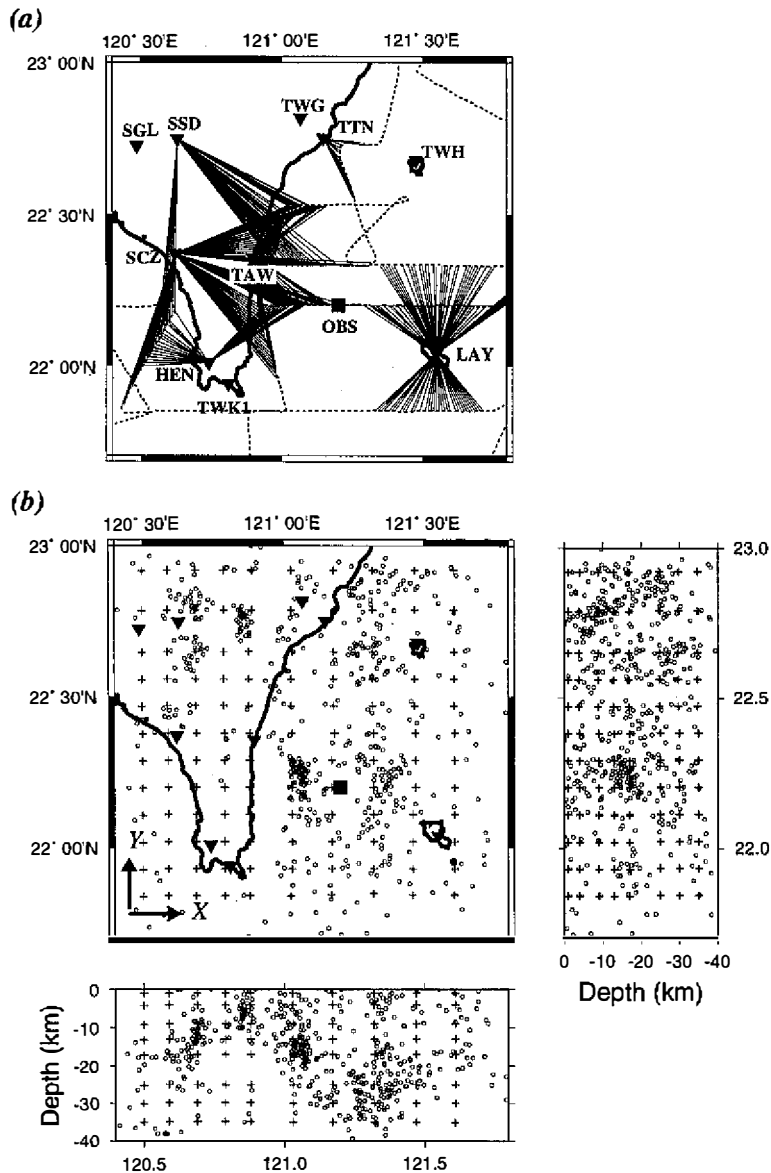


Fig. 2. Ray paths for air-gun shots and initial locations of events used in inversion process. (a) Solid lines and dashed lines indicate ray paths of air-gun shots and ship tracks of R/V Maurice Ewing survey conducted in September 1995, respectively. Inverted triangles indicate stations of Central Weather Bureau Seismographic Network (CWBSN). Solid square represents ocean bottom seismometer (OBS). CWBSN stations are labeled. (b) Grid used for velocity inversion (pluses), earthquakes (circles), and stations in southeastern Taiwan area.

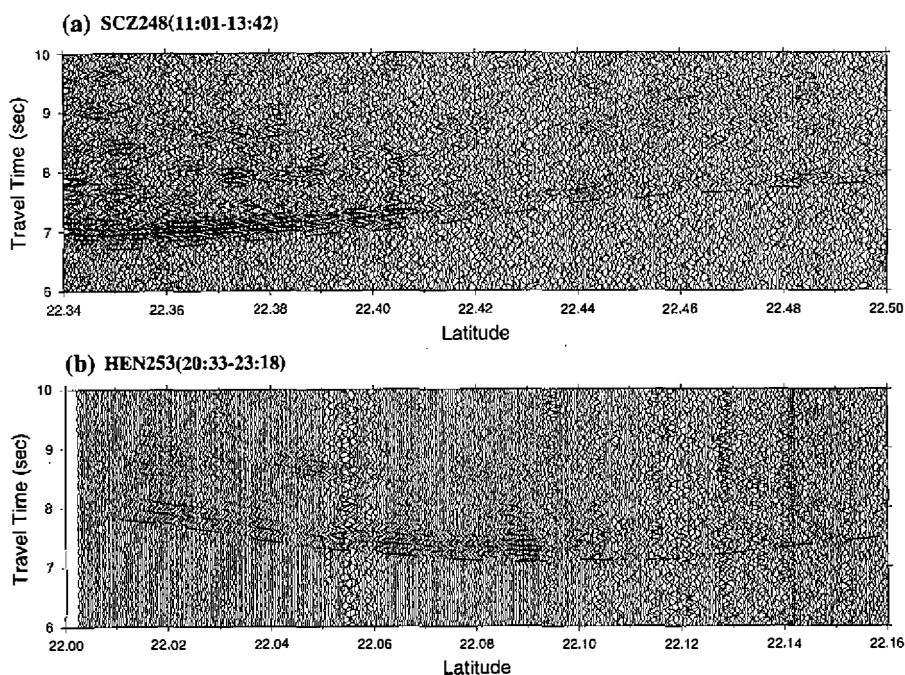


Fig. 3. Seismic sections recorded by CWBSN station SCZ (a) and HEN (b). Dotted lines represent the first arrival times. Average intervals of recorded traces are about 50 meters.

To refine the hypocenter of earthquakes and determine a more reliable one-dimensional (1-D) velocity model for the study area, the VELEST program (Kissling *et al.*, 1994) was run with two distinctive different 1-D velocity models. The first velocity model was modified from Chen (1995), who inverted earthquake arrival time data for the 3-D velocity model and station correction for the Taiwan region. This velocity model has a thicker middle- and lower-crust (Figure 4a). Alternatively, based on seismic refraction studies (Chen *et al.*, 1995; Lin *et al.*, 1997a), the model has proposed that the Moho depth is 35 km beneath the Henchun Peninsula and that this decreases eastward to about 12 km beneath Lutaio island and less than 10 km beneath the Philippine Sea. This means that the study area should be an arc region or a transition from a continental-like crust to an oceanic-like crust. So another model, namely the “arc model”, based on the profile crossing the Kyushu-Palau ridge (Ludwig *et al.*, 1973) was introduced. After 3 iterations in running VELEST program, a “preferred model”, with a significantly smaller data variance and RMS residual than the “arc model”, is obtained for the 1-D initial model (Figure 4a).

In Figure 4a, the 1-D “preferred model” seems to have a very low V_p below 30 km in depth which is lower than that for a typical continental mantle. We do not know what the “normal” mantle velocity structure beneath the study area is. However, we can think of two possible explanations of the inversion result for low V_p . First, it could be a reliable result that

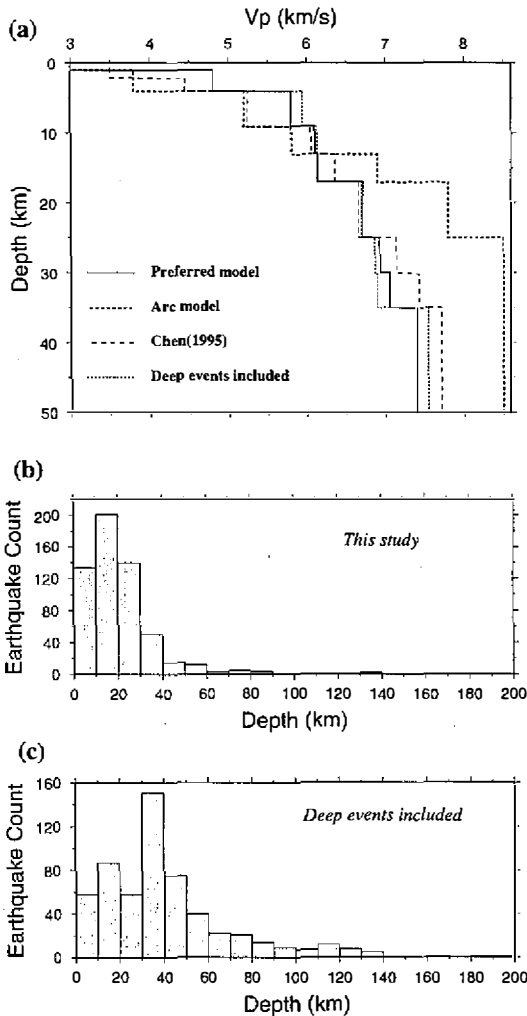


Fig. 4. (a) Both the “preferred” V_p (solid line) models determined using crustal earthquakes or data set including deep events (dotted line), show lower mantle velocities feature. “Arc” model (Ludwig *et al.*, 1973) and initial model (Chen, 1995) in running VELEST program are also shown. Histogram of earthquake counts as function of depth for this study (b), and including deeper events (c), used in running VELEST program are shaded.

represents the “normal” structure in this area. Alternatively, the low velocities may result from the insufficient ray coverage below 30 km in depth that would not affect the initial model during inversion. As mentioned in the previous section, the hypocentral depth of the selected events are mostly crustal earthquakes (Figure 4b). For the purpose of checking the travel times of the deeper events would result in a different 1-D velocity solution, the other data set including deeper events was used (Figure 4c). Both the mantle velocity deduced here using the crustal events and that deduced using deeper events tend to exhibit features of low velocity ($V_p < 7.6$ km/s). The results of the 1-D inversion therefore imply the existence of some thickness of low-velocity material within the upper mantle (see also Roecker *et al.*, 1987).

Successive inversion processes are carried out by decreasing the grid spacing from a coarse to a fine grid in the study area. The model calculated at each step is used as the input model for the following inversion. We performed a trade-off analysis (Eberhart-Phillips, 1986) of the

data and the model variances in order to choose the most suitable damping parameter to be used in the damped least-squares inversion. Finally, we used a horizontal grid spacing of 10 km on land and 15 km in the offshore area. The grid area extended 115 km east-west and 120 km north-south (Figure 2b). A damping value of 30 has been chosen as an optimum trade-off between data and model variances.

4. RESULTS

4.1 Preferred Vp Model

Figure 5 shows horizontal slices taken from the 3-D velocity solution. The 3.0 and 4.0 contours for the spread function contours (Backus and Gilbert, 1967; Menke, 1989; Michelini, 1991) outline the well resolved parts of the model.

At the 4-km depth, the Vp has an average value of 5.74 km/s. A good correspondence of velocity to the known structure is evident, with higher velocities occurring in the Central Range and on Lanhsu island (Figure 5a). The southern part of the Hengchun peninsula, the Huatung Ridge and the Taitung Trough all have relatively low Vp at the 4-km depth. The near-surface low Vp features of these areas coincide with the observation of sediment deposition shown in surficial geology (Ho, 1986) and offshore reflection profiles (Fuh *et al.*, 1997). One of the prominent features of the Vp structure is a sharp velocity contrast along the trace of the Longitudinal Valley Fault and coastal line shown in the 4-km, 13-km and 17-km depth interval. The spreading function indicates high resolution for the velocity contrast. Below the 25-km depth, velocities are poorly resolved (Figure 5).

The 3-D velocity structure is also displayed in Figures 6 and 7 as a series of cross-sections, arranged from north to south and from west to east, respectively. The most striking feature is the large, N-S elongated high-velocity zone beneath the Southern Longitudinal Trough and Huatung Ridge of the model, seen best in Figures 6a-6c. Well-resolved velocities within the high velocity zone are much higher than both the portion of the Central Range and the Luzon arc in the middle crust. If we use the 6.5 and 7.0 km/s contours as the boundary of the high velocity zone, it may extend to at least 20 km in depth in our model (Figures 6b and 6c).

The major feature of the south-north cross-sections is that the crust of the central Hengchun peninsula is thicker between 22.2° N and 22.6° N than in southern or northern adjacent parts (Figure 7a). The lateral velocity variation is very clear near the Taitung Canyon (Figure 7c). In general, the 3-D velocity solution shows the complexity of the velocity pattern from south to north.

4.2 Solution Quality

We measure the solution quality by estimating the picking error, computing spread function, model standard error, and through comparisons of inversions with synthetic data. We first check whether the high velocity volume beneath the Southern Longitudinal Valley and Huatung Ridge (Figure 6b) can be attributed to the error in picking arrivals. The grid point within the high velocity body was chosen as the center of a sphere with a 10-km radius. The residuals of the rays crossing this sphere were calculated. We find that there are 103 positive

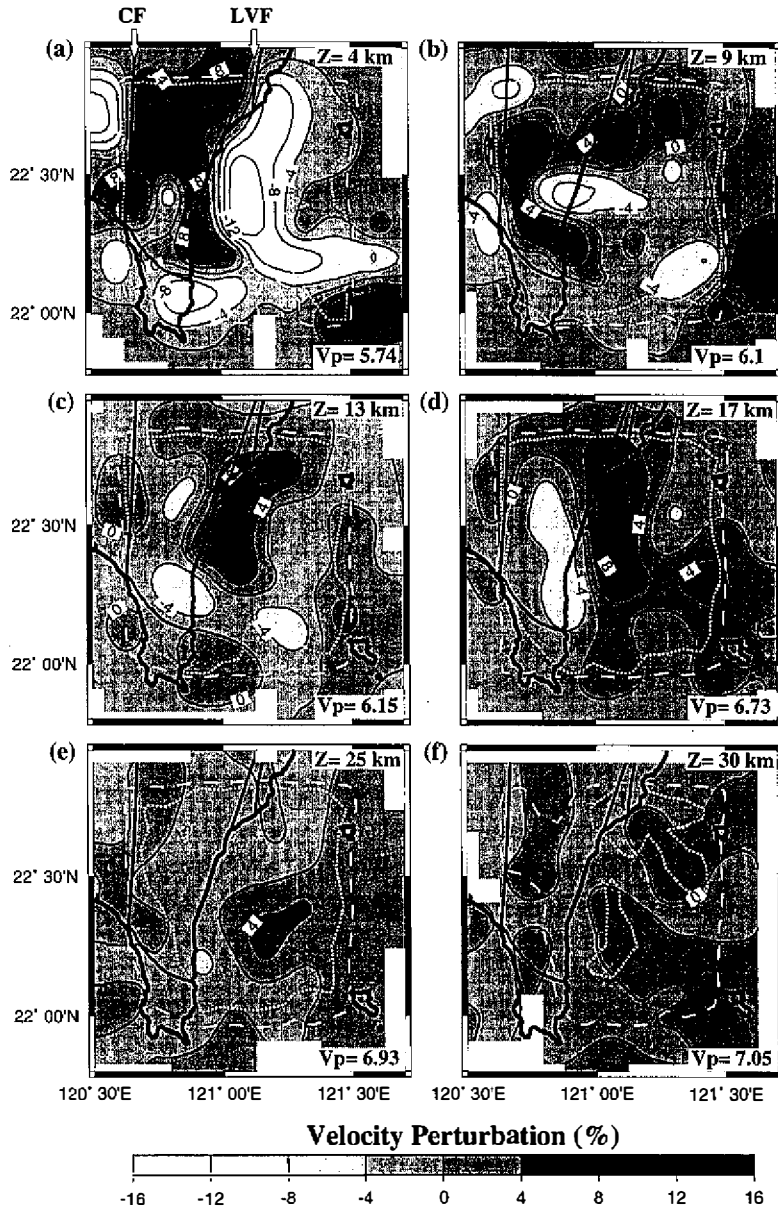


Fig. 5. Velocity perturbation solution of 3-D velocity solution in map-view at six depth slices at 4, 9, 13, 17, 25 and 30 km. See Figure 2 for reference map. Major faults and spread function for 3.0 (dotted white lines) and 4.0 (dashed white lines) are also shown. Spread function smaller than 3.0 indicates velocity value is well-resolved and spatially well-constrained. Average velocity for each depth slice is shown in right-lower corner. (LVF: Longitudinal Valley Fault; CF: Chaochou Fault).

and 112 negative residuals that were contributed by a wide azimuth of rays. This means that the picking error should not affect the model. Secondly, the model solution profiles along Figure 6b for various damping values also indicate that the existence of the high velocity is essential. We use the spread function of each averaging vector rather than the diagonal elements of the resolution matrix to evaluate how well the model parameters are resolved (Toomey and Foulger, 1989; Michelini and McEvilly, 1991). The smaller the value of the spread function, the more compact the averaging vector and the better the volume averaging is centered on the respective grid point (Eberhart-Phillips and Michael, 1993; Hauksson and Haase, 1997). The spread function contours show that most parts of the model are well solved down to a depth of 25 km (Figure 5). At the same time, we use the model standard error to provide an estimate of the mapping of the data error into the model error. We found that the standard error determined from the covariance matrix varies throughout the model ranging from 0.02 to 0.05 km/s.

To evaluate how the actual ray coverage allows us to resolve the complex crustal structure beneath the area studied, we also perform a synthetic test called “restoring resolution test” (Zhao *et al.*, 1992). This test uses the velocity model obtained by inverting the real data sets as the synthetic model, and then the synthetic travel times are computed from the synthetic model using the same sources and receivers used for the real data sets. After adding a random noise in a normal distribution to the synthetic travel time data, we inverted the synthetic data with a homogeneous starting model. In this study, a random noise with standard deviations of 0.05 s, 0.1 s, 4 km, and 4 km were added to the P travel times, origin times, and horizontal and vertical hypocentral locations for the synthetic data, respectively. The result shows that the high velocity anomalies mentioned above have been recovered in the central part of the model.

5. DISCUSSION

5.1 Interpretation of Crustal Structure and Rock Units

The overall shape and location of shallow velocity features correspond well to the mapped surface geology. However, the deeper subsurface structure is much more complex than their physiographic expression would suggest.

The southern Central Range, bounded by the PLVF and Chaochou Fault, shows a relatively high velocity zone (4–12% higher than at 5.74 km/s) extending from the surface to about 9 km in depth in the 3-D solution. This high velocity feature seems to end near 22.2° N (Figures 5a and 5b). The surficial high velocity stratum of the southern Central Range dips eastward to the offshore area near 22.5° N, which is generally consistent with the refraction study by Cheng *et al.* (1996b).

Although the main volcanic activity ceased in the middle Miocene in this part of the Luzon arc, magmatic activity may have left a strongly heterogeneous and irregular structure owing to the presence of magmatic intrusions and magma chambers that have cooled and solidified. The most obvious feature is the lenticular bodies shown in Figures 6a and 6f, with velocities ranging from 4 to 6 km/s, that are associated with Lutao and Lanhsu. The depth of the 6 km/s contour line is about 15 km. Since we have only a weak image between 20 and 30 km in depth, the 3-D velocity model can't indicate the Moho depth beneath Lutao and Lanhsu.

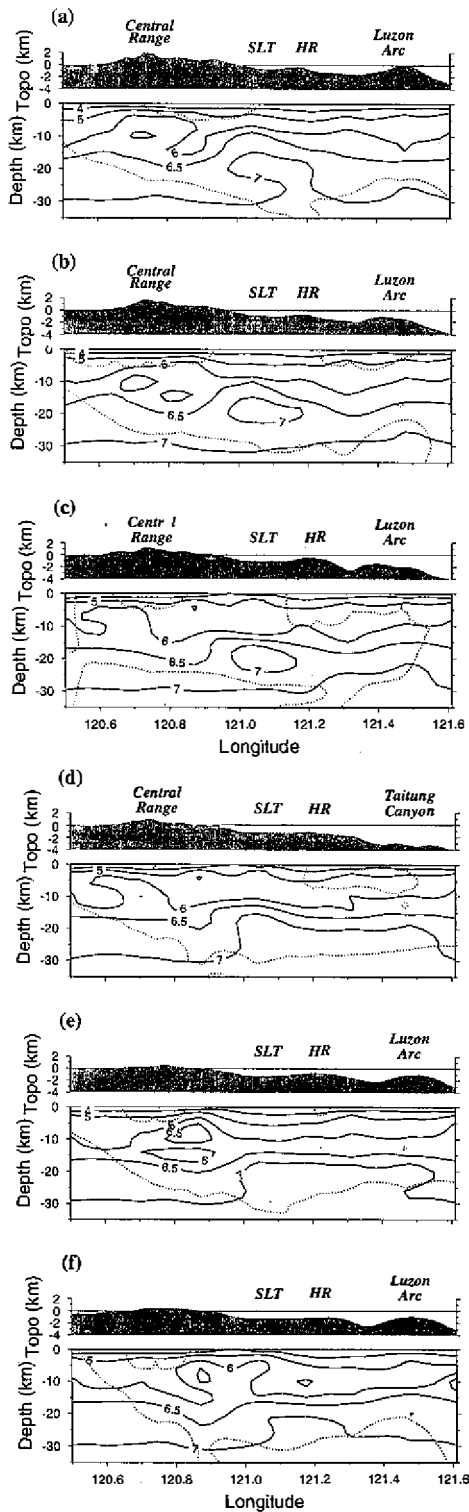


Fig. 6. Cross-sections of 3-D velocity solution from (a) 22.65° N to (f) 22.20° N. V_p contoured at 0.5 km/s intervals. Topography of each cross-section is shown on top. Spread function for 3.0 (dotted gray lines) is shown for each section. Most of our study region is well-resolved and spatially well-constrained. (SLT: Southern Longitudinal Trough; HR: Huatung Ridge).

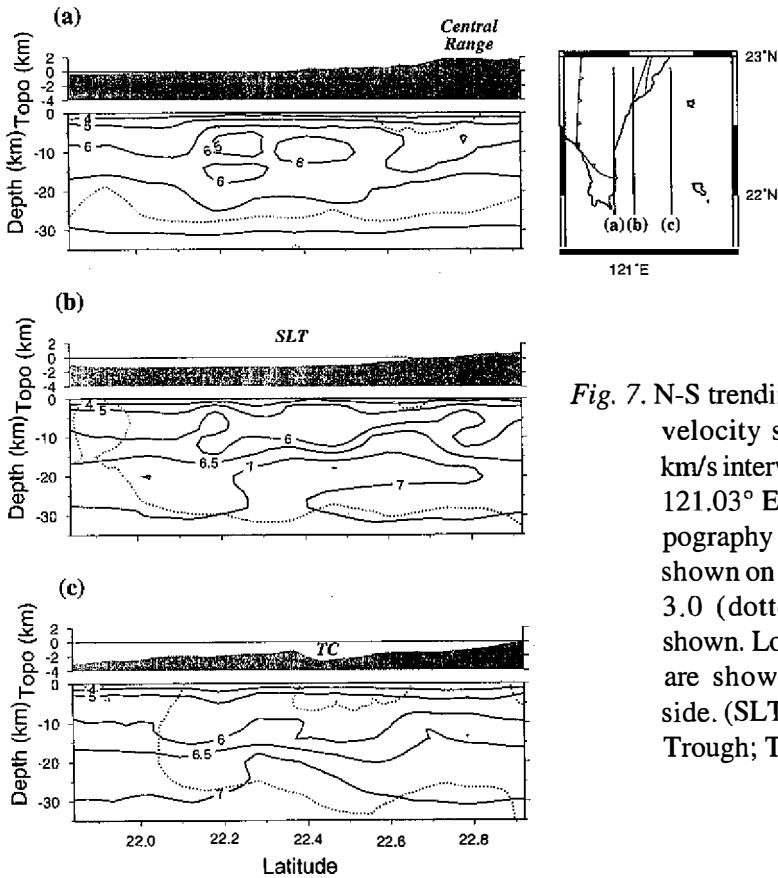


Fig. 7. N-S trending cross-sections of 3-D velocity solution contour of 0.5 km/s intervals for (a) 120.88° E, (b) 121.03° E, and (c) 121.32° E. Topography of each cross-section is shown on top. Spread function for 3.0 (dotted gray lines) is also shown. Locations of cross sections are shown on upper right-hand side. (SLT: Southern Longitudinal Trough; TC: Taitung Canyon).

It is worth noting that there is a high velocity uplift beneath the Taitung Canyon (Figure 7c). Located within the Lutaο and Lanhsu volcanic islets, the high velocity uplift could represent the normal oceanic crust which has a relatively high velocity in the middle crust. However, the spatial distribution of the high velocity uplift does not support this. Alternatively, according to the paleomagnetic study of the Coastal Range, the Luzon arc has been segmented and rotated clockwise for each segments during the oblique collision of the Eurasian and Philippine Sea plates (Lee *et al.*, 1991). This means that the segmentation and rotation has taken place between Lanhsu and Lutaο. We thus suspect that the high velocity uplift beneath the Taitung Canyon might be associated with zones of solidified intrusives in consequence of arc segmentation by a major stress difference near the Taitung Canyon (Hsu and Sibuet, 1995; Shyu *et al.*, 1996).

One of the goals of this study was to image structures such as the southward extension of the Longitudinal Valley Fault. In order to describe the lateral variation in a more systematic manner, the velocity contrast within each layer was calculated. Figure 8 shows that the southern prolongation of the Longitudinal Valley Fault (PLVF), characterized by a sharp velocity contrast, is the primary feature in the velocity model. The southern end of the PLVF could be traced to at least 22.38° N.

5.2 The High Velocity Body (HVB)

To the east of the PLVF, an elongated high velocity anomaly (compared with the material to the west of the fault) is observed in the middle- to lower-crust beneath the Southern Longitudinal Trough and Huatung Ridge (Figure 6). In a convergent zone, the existence of such a high velocity volume is not unusual (e.g., Langston, 1981; Spence *et al.*, 1985; Fuis *et al.*, 1991). Based on the distribution of its velocity and depth, the HVB might be an oceanic or mafic material. However, it seems exotic, relative to the surrounding low velocity portions. Cheng *et al.* (1997) have traced this high velocity body to at least 24° N, as deduced from local earthquake tomographic inversion.

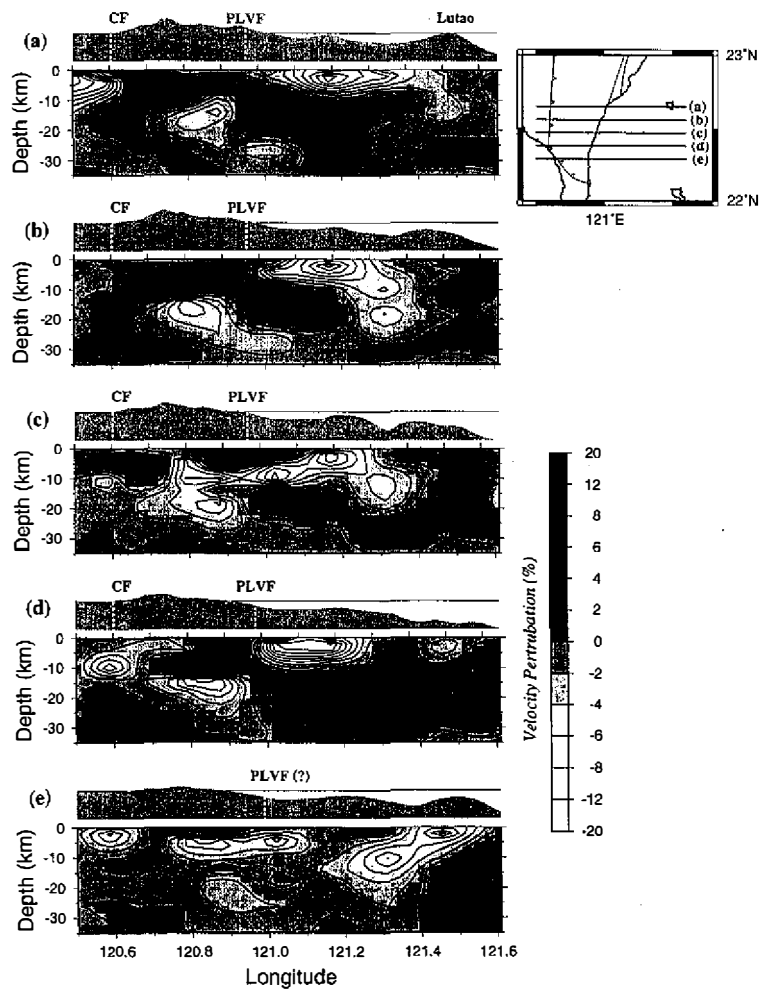


Fig. 8. Velocity perturbation cross-sections illustrating southern prolongation of Longitudinal Valley Fault (PLVF) along five profiles shown top right. Velocity perturbation range from -20% to +20%. (CF: Chaochou Fault).

In order to estimate the possible rock source of the HVB, we compared the depth-velocity profile of the HVB with the measured wave velocities of rocks under specific pressure-temperature conditions reported in the literature (Christensen, 1965; Kern, 1978; Christensen, 1979; Christensen and Mooney, 1995). Because the crustal geothermal structure is important for the interpretation of seismic velocity distribution, we first constructed the temperature-depth model for the study area based on the six thermal gradient values in southern Taiwan area reported by Lee and Chang (1986). Assuming that the temperature increases linearly with depth, the estimated temperature-depth curve (curve "south" in Figure 9a) is significantly higher than that of the continental crust (curve "C" in Figure 9a). Since there are no experimental data for the temperature/pressure function for the rocks in southeastern Taiwan, we have therefore used the experimental P-wave velocities of many rocks, collected by Christensen and Mooney (1995) at specific temperature-depth relation (curve "C" in Figure 9a), to estimate the possible composition of the HVB. When we superposed the velocity-depth distribution of the HVB on those from Christensen and Mooney (1995), it shows that several rocks (e. g., Granite-Norite-Troctolite, Amphibolite, Mafic Granulite) are located within the velocity range of the HVB in the 13- to 25-km depth range (Figure 9b). This suggests that the HVB might be a mixture of igneous and low- to medium-grade metamorphic rocks.

There are several possible explanations for the existence of the HVB at middle and lower crustal depths. The first is that it has been upthrust from the oceanic crust of the Philippine Sea plate or from below the Luzon arc basement. The second is that the HVB of the Philippine Sea plate has been brought into its present position by left lateral displacement at the Longitudinal Valley Fault. The third explanation, proposed by Lin *et al.* (1997b), is that it is caused by the ongoing exhumation of previously subducted continental crust. This might be an appropriate model for a high-compression region, such as the Hualien area. For the pre-collision stage of southeastern Taiwan, it is not known whether the mechanism of crustal exhumation has taken place. The fourth, proposed by Cheng *et al.* (1997), is that the HVB may be related to the remnant oceanic crust of the old Philippine Sea plate (Sibuet and Hsu, 1997) during the collision of the former south Ryukyu arc and the Luzon arc. Finally, the HVB could correspond to the oceanic crust beneath the forearc basin which was torn off and separated from the Philippine Sea plate after the Luzon arc was formed, and has been shortened during the collision of the Eurasian and Philippine Sea plates. Based on seismic refraction studies, the Moho depth is about 35 km beneath the Hengchun peninsula (Lin *et al.*, 1997b) and about 31 km for the oceanic arc (Mooney *et al.*, 1998). As shown in Figure 6, when compared with the Luzon arc and the Central Range on either side of it, the forearc crust shows the feature of relatively high velocity in the middle crust. Thus, the spatial distribution of the HVB (Cheng *et al.*, 1997), the forearc basin structure (e.g., the Huatung Ridge and the thick sediments above the HVB shown in Figure 6) and the possible composition of the HVB mentioned above all support the last explanation.

5.3 Gravity Modeling

Modeling of gravity data constitutes an important check on the tomographic inversion results and enables estimation of crustal densities. Figure 10a shows the E-W trending magnetic and Bouguer gravity profiles close to Taitung Canyon (22.38° N) compiled by Liu *et al.*

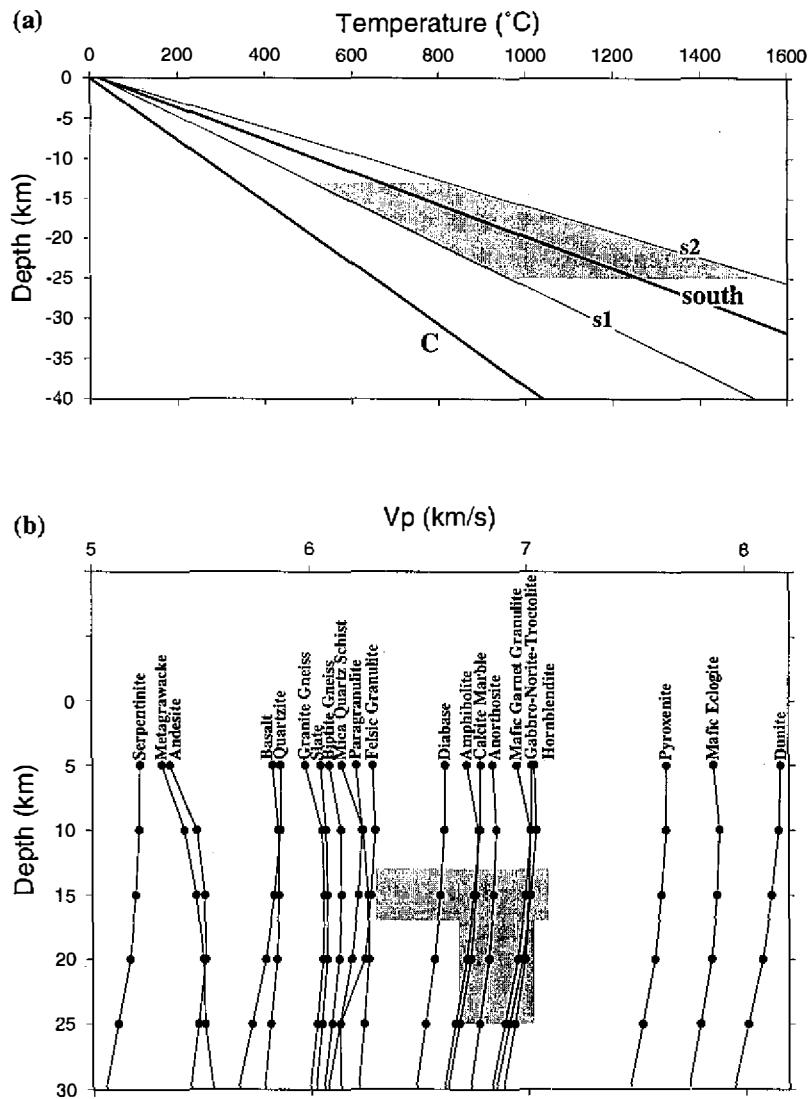


Fig. 9. Temperature-depth functions and laboratory measured velocities in major rock types. (a) Temperature-depth curve (curve "south") for onshore-offshore area of southeastern Taiwan calculated with thermal gradient values from Lee and Chang (1986). Shaded area represents depth distribution of high velocity body (HVB) beneath Southern Longitudinal Valley and one standard deviation (curves "s1" and "s2"). Temperature-depth function (curve "C") used in laboratory measured velocities for major rock types shown in (b). (b) Velocity-depth distribution of HVB (shaded area) compared to average laboratory measured velocities in major rock types reported by Christensen and Mooney (1995).

(1992). The Bouguer gravity exhibits a major negative anomaly between 121° E and 121.4° E. The landward gradient near 121° E requires a relatively sharp density contrast within the basement. In the eastern part, the seaward gravity gradient near 121.5° E is mainly related to the Luzon arc that is also indicated by the magnetic data.

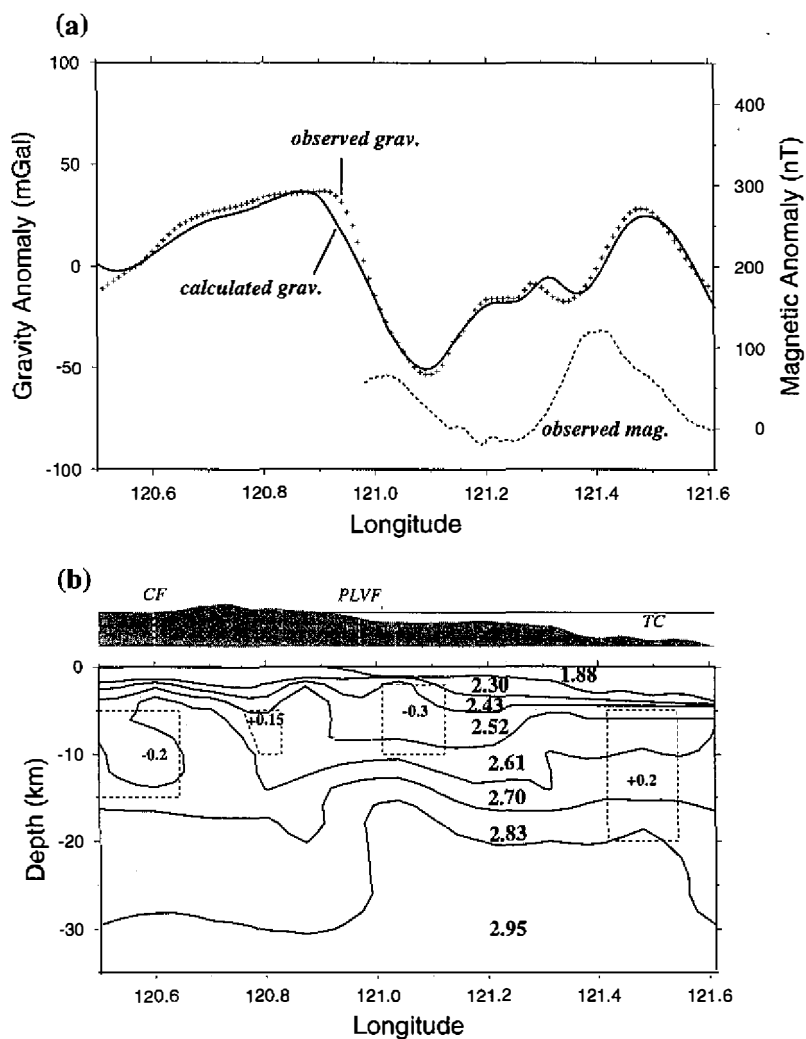


Fig. 10. (a) Observed and calculated gravity along profile 22.38° N. Dashed line indicates observed magnetic data. (b) Density model to calculate gravity anomaly curve shown in (a) with densities in Mgm^{-3} . Topography of observed section is shown on top. Note dashed blocks representing added volumes with density contrast. See text for explanation. (PLVF: the southern prolongation of the Longitudinal Valley Fault; CF: Chaochou Fault; TC: Taitung Canyon).

The seismic velocities along the 22.38° N section (Figure 6d) were divided into several horizontal prisms with simple polygons. The velocities of each prism were taken from the mean values of the velocity of the top and bottom interfaces. The velocities were then converted into densities (Figure 10b) using the linear relationship from Barton (1986). In modeling, the water volume was replaced by sedimentary material with a density of $1.88 \text{ (M gm}^{-3}\text{)}$. After adding 4 blocks of density contrast, the fit between the observed and calculated Bouguer gravity anomalies is good, and any misfit in an individual point is generally less than 10 mGal. Although the calculated gravity anomalies is only one possible solution, the several blocks added still give us some idea of the real structure. For instance, the block with a value of +0.2 near the Taitung Canyon might indicate the existence of a thinner crust beneath the Taitung Canyon rather than the feature shown in Figure 6d. On the other hand, the blocks with values of -0.3 and -0.2 located close to the PLVF and CF, respectively, imply that a thicker sedimentary layer beneath the Southern Longitudinal Valley and Pingtung plain, respectively, should be considered.

5.4 Seismicity and Focal Mechanism

The 3-D velocity model obtained in this study was used to relocate 1899 earthquakes that occurred inside the boundaries of the model between January 1990 and May 1997. The travel time data for P and S waves were selected from the CWBSN catalog. Compared to the hypocentral results of the catalog, the weighted root mean square (RMS) arrival time residuals of the relocated events were reduced from 0.29 to 0.147 seconds. From the seismicity of widespread, scattered earthquakes that occurs in the entire southeastern Taiwan area (Figure 11a), it seems that the Taitung Canyon is likely to be aseismic, and marks the boundary between the different background seismicity of the northern and southern parts of the region. When a 20-km width of seismicity was projected onto the 22.65° N and 22.2° N velocity perturbation cross-sections, the hypocenters concentrated at the edges of larger V_p contrasts (Figure 11b and 11c). This is consistent with the observations that the earthquakes occur within high V_p/V_s zones or adjacent to high V_p bodies (Michael and Eberhart-Phillips, 1991; Eberhart-Phillips and Michael, 1993; Thurber *et al.*, 1997; Hauksson and Haase, 1997).

Also shown in Figure 11b and 11c, a notable feature of the seismicity distribution beneath southeastern Taiwan is the three N-S trending earthquake activity zones: from east to west, the seismic zones beneath the Taitung Trough, the PLVF and the Chaochou Fault (Figure 11a). In addition, it is likely that if the PLVF and Chaochou Fault are traced from cross-sections 22.2° N to 22.65° N, a left-lateral offset across the Taitung Canyon will be found (Figures 11b and 11c).

Figure 12 shows the location and focal mechanism of moderate earthquakes with hypocenter depths of less than 35 km, as determined by Lin and Tsai (1981), Cheng (1995), Ma, K. F. (1997, personal communication), Huang (1997) and this study. Although many local variations occur (Cheng, 1995; Huang, 1997), focal mechanisms indicate two types of faulting, the strike-slip and upthrust. The upthrust earthquakes with an east-west trending of the upthrust fault and with a small strike-slip component are mainly located along the Taitung Trough (*e.g.* Earthquake Nos. 19, 9, 12, 1 and 4). In addition, the focal mechanism of the events that oc-

curred along the PLVF are characterized by N-S trending left-lateral strike-slip faulting (e.g. Earthquake Nos. 8, 11 and 18). There are a few large events that occurred near the Taitung Canyon which show that a northeast-southwest trending of strike-slip faulting dominates (e.g. Earthquake Nos. 2, 3, 6 and 7). If we trace the bathymetry contour lines for the Taitung Canyon, it seems to extend westwards from 122.5° E to 121.2° E (Figure 12). We have no information about the velocity model of the Taitung Canyon east to the Luzon arc. However, the westward extension of the Taitung Canyon into the Luzon arc and its relation to the high-velocity uplift shown in Figure 7c, remains an important objective of future research.

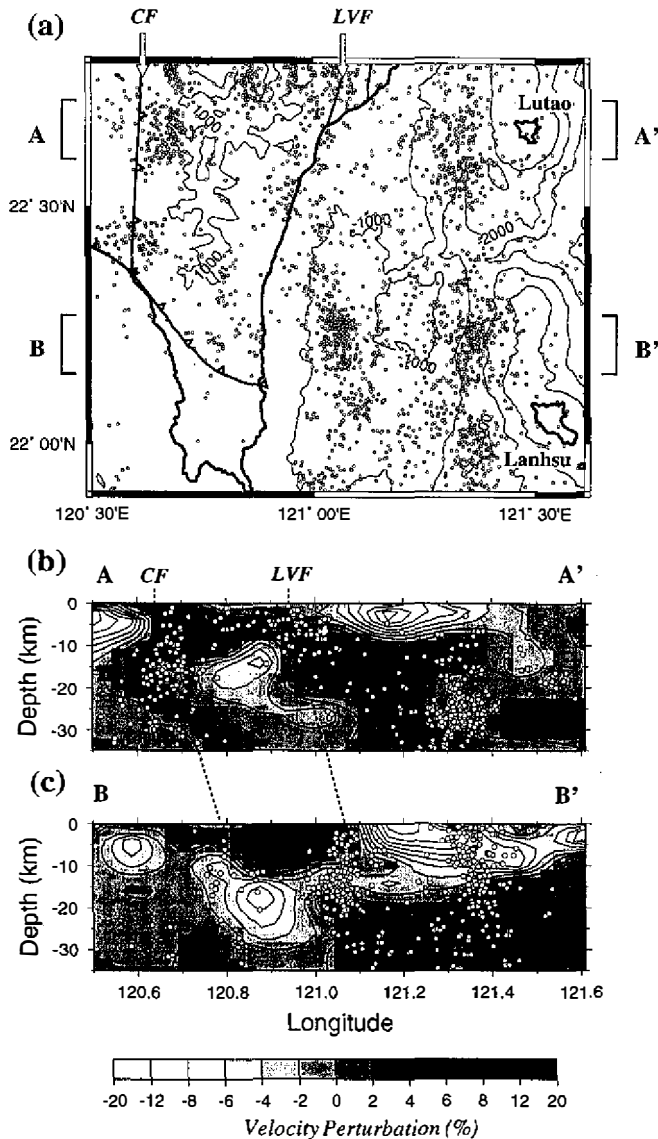


Fig. 11. Relocated seismicity for 1990 to 1997 in (a) map-view at surface, and superposed on velocity perturbation cross-section along (b) 22.65° N (AA') and (c) 22.20° N (BB'). Note hypocenters shown in (b) and (c) tend to be at locations where there is a greater gradient in Vp model. (LVF: Longitudinal Valley Fault; CF: Chaochou Fault).

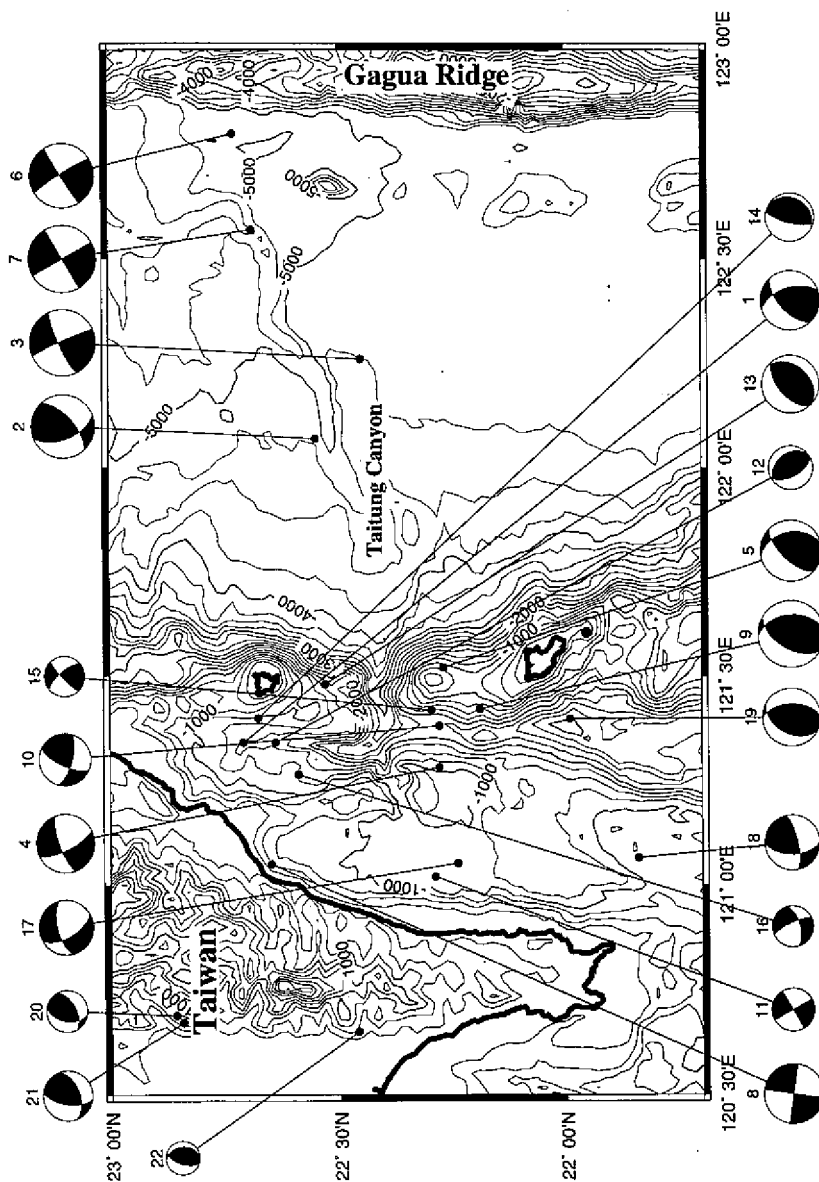


Fig. 12. Map showing epicenter and focal mechanism of moderate earthquakes near study area. Fault plane solutions are plotted in equal-area projections of the lower hemispheres of focal spheres. Compressional quadrants are shaded. Earthquake numbers are labeled on top. Note events occurring near the Taitung Trough show mainly thrust-fault solutions, while those along PLVF and Taitung Canyon indicate mostly strike-slip solutions.

5.5 Implication for Regional Tectonics

For the purpose of understanding the dynamics of plate interaction, such as crustal deformation, we have superposed the 3-D velocity solution in map-view at a depth of 4 km on the offshore structural map from Fuh *et al.* (1994), along with the geodetic velocity field by Yu *et al.* (1997). Figure 13 shows that the major surficial faults are situated within the surficial low velocity layers, illustrating how the shallow Central Range and Luzon arc high velocity volumes play an important role in the deformation of the offshore sedimentary layers in the study area. For instance, the sharp strike change of the faults to the south of Tawu is coincident with the strong material represented by both the magnetic high (Shyu and Chen, 1991) and the high velocity zone in the 3-D Vp model. Moreover, the geodetic velocity field also reveals a large decreasing of velocity magnitude from east to west in the study area (Figure 13). The geodetic velocity ratio of the Luzon arc, the forearc portion and the Central Range zones is 2.5:2:1.

Taken together, the above observations suggest the possibility of roughly dividing the southeastern Taiwan area into three sub-areas: the Luzon arc, the Central Range and the forearc area in between (Figure 14). These sub-areas can be delineated by two faults, the PLVF to the west of the forearc area, and the Taitung Trough Fault to the east. It has been recognized that moderate earthquakes recur along the same segments of some faults. The clearest example of this repeating behavior can be found along the San Andreas Fault (Bakun and Lindh, 1985). In southeastern Taiwan, it is not known whether such a condition on potential earthquake nucleation sites would still hold. However, based on the seismicity and focal mechanisms shown in Figures 11 and 12, it is possible that the PLVF and Taitung Trough Fault are the potential sites of future moderate earthquakes.

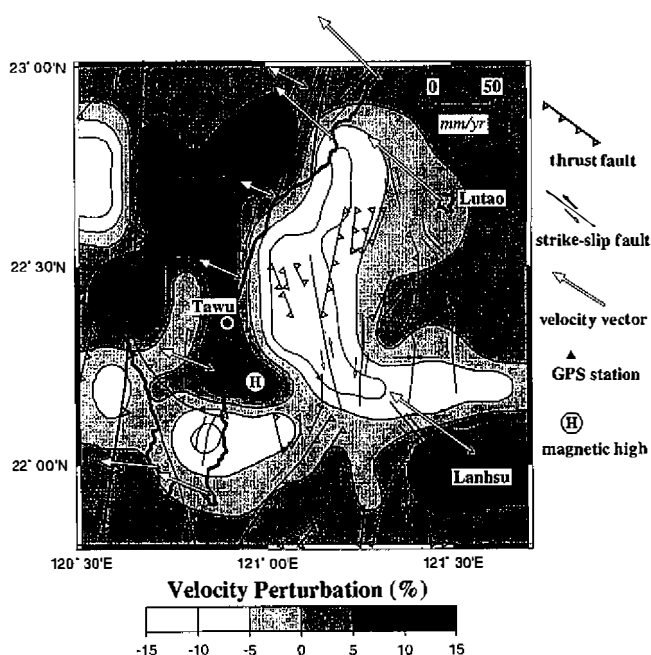


Fig. 13. Velocity perturbation in map-view at 4-km depth from 3-D solution and surficial fault distribution. Geodetic velocity field (Yu *et al.*, 1997) is also shown. Offshore data are inferred from Fuh *et al.* (1994) using seismic reflection. Velocity variation scale is shown at bottom, while the geodetic velocity scale is shown top right. See text for explanation.

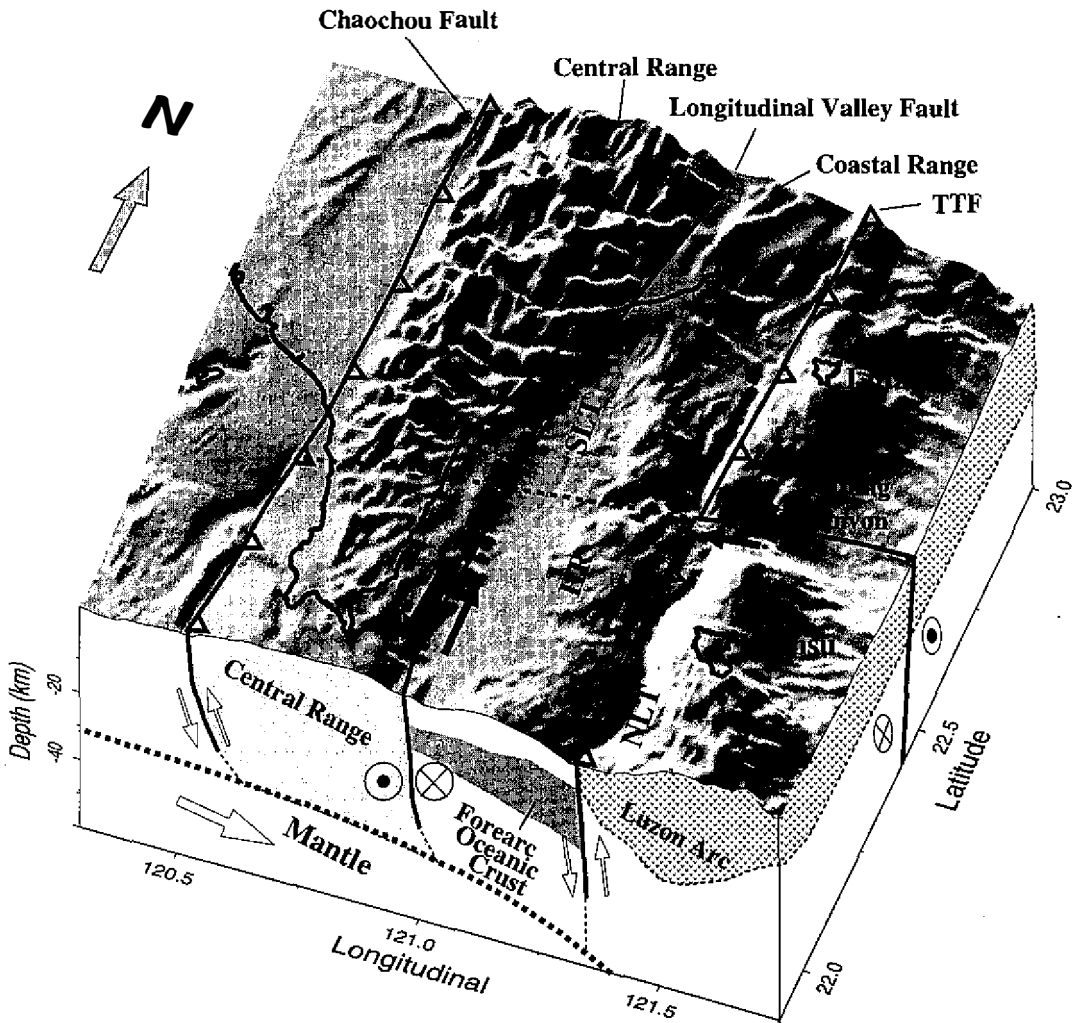


Fig. 14. Schematic block diagram summarizing crustal structure and faulting geometry inferred from tomographic inversion and relocated seismicity in this study. Shaded perspective-bathymetric diagram of the southeastern Taiwan area is also shown. View is taken from south-southeast. Central Range, forearc area and Luzon arc are distinguished roughly by three seismicity-defined faults: Chaochou Fault, Longitudinal Valley Fault and Taitung Trough Fault (TTF). Note Taitung Canyon manifests itself as strike-slip fault, but its westward extension is not clear. (SLT: Southern Longitudinal Trough; HR: Huatung Ridge; TT: Taitung Trough).

6. CONCLUSIONS

- (1). Based on velocity structure and focal mechanisms, we divide the southeastern Taiwan area into three main distinct deformation sub-areas : the Luzon arc in the east, the Central Range in the west and the forearc area in between. These sub-areas are defined by two faults, a strike-slip fault (the southern prolongation of the Longitudinal Valley Fault) to the west of the forearc area, and an upthrust fault (the Taitung Trough Fault) to the east. The surficial fractures or faults are mostly within the upper crust of the forearc area that has lower velocity.
- (2). There is a large volume of high velocity material, which should be a mixture of igneous and low- to medium-grade metamorphic rocks, beneath the forearc area. The high velocity body can be interpreted as the forearc oceanic crust of the Philippine Sea plate which was torn off and separated from the Philippine Sea plate after the Luzon arc had been formed, and has been shortened during the collision of the Eurasian and Philippine Sea plates.
- (3). The southern prolongation of the Longitudinal Valley Fault is the primary feature in the 3-D velocity model obtained from inversion of P wave arrivals from local earthquakes and air-gun shots. A clear and sharp lateral velocity variation is seen across the fault at various sampled depths and can be traced southwards to at least 22.38° N.
- (4). At the southern end of the eastern flank of the Central Range, a high-velocity structure is found from the surface to about 9 km in depth beneath the northern part of the Hengchun peninsula. This structure seems to end near 22.2° N where it turns eastwards to the offshore area.
- (5). From the distribution of relocated hypocenters between January 1990 and May 1997, the Taitung Canyon seems to mark a boundary between different background seismicities. In addition, the high velocity uplift beneath the Taitung Canyon might be associated with zones of solidified intrusives in consequence of the arc segmentation due to a major stress difference between the islets of Lanhsu and Lutaou.
- (6). We also found that the relocated hypocenters are mostly concentrated at the locations where V_p has a greater gradient. This implies that earthquakes mainly occur at the edge of areas that behave as rigid blocks.

Acknowledgments The authors are grateful to the Seismological Observation Center, Central Weather Bureau, for providing data on earthquakes and air-gun shots and to the TAICRUST group for providing the air-gun sources. We benefited from discussions with L. -Y. Chiao of the Institute of Oceanography, National Taiwan University, C. -H. Lin and R. -J. Rau of the Institute of Earth Sciences, Academia Sinica, and K. -F. Ma and S. -K. Hsu of the Institute of Geophysics, National Central University. Thanks are also due to the members of the Institute of Earth Sciences, Academia Sinica for their efforts in recording the air-gun data. The anonymous reviewers have greatly improved the manuscript. This study was supported by the National Science Council of the R.O.C.

REFERENCES

- Backus, G., and F. Gilbert, 1967: Numerical applications of a formalism for geophysical inverse problems. *Geophys. J. R. astr. Soc.*, **13**, 247-276.
- Bakun, W. H., and A. G. Lindh, 1985: The Parkfield, California, earthquake prediction experiment. *Science*, **229**, 619-624.
- Biq, C., 1972: Dual-trench structure in the Taiwan-Luzon region. *Proc. Geol. Soc. China.*, **15**, 65-75.
- Barton, P. J., 1986: The relationship between seismic velocity and density in the continental crust - a useful constraint ?. *Geophys. J. R. astr. Soc.*, **87**, 195-208.
- Bowin, C., R. S. Lu, C. S. Lee, and H. Schouten, 1978: Plate convergence and accretion in the Taiwan-Luzon region. *Am. Assoc. Pet. Geol. Bull.*, **62**, 1645-1672.
- Cardwell, R. K., B. L. Isacks, and D. E. Karig, 1980: The spatial distribution of earthquakes, focal mechanism solutions, and subducted lithosphere in the Philippine and northeastern Indonesian islands. In: D. E. Hayes (Ed.), *The Tectonic and Geologic Evolution of Southeast Asian Seas and Islands*, American Geophysical Union, geophysical monograph 23, 1-35.
- Chai, B. H. T., 1972: Structure and tectonic evolution of Taiwan. *Am. J. Sci.*, **272**, 289-442.
- Chang, C. P., 1996: Geological relationship between the Lichi melange in the Coastal Range and the Huatung Ridge in the active collision zone off southeastern Taiwan. Master's Thesis, National Taiwan Univ. 120 pp. (in Chinese)
- Chen, A. T., Y. Nakamura, and C. S. Liu, 1996: Crustal structure in eastern offshore of Hengchun Peninsula. The Sixth Taiwan Symposium on Geophysics, Chia-Yi, Taiwan, 555-560.
- Chen, M. P., and W. S. Juang, 1986: Seafloor physiography off southeastern Taiwan. *Acta Oceanogr. Taiwanica*, **16**, 1-7.
- Chen, Y. L., 1995: Three dimensional velocity structure and kinematics analysis in Taiwan area. Master's Thesis, National Central Univ. 172 pp. (in Chinese)
- Cheng, S. N., 1995: The study of stress distribution in and around Taiwan. Ph.D. thesis, National Central Univ. 215 pp. (in Chinese)
- Cheng, W. B., C. Wang, and C. T. Shyu, 1996a: Crustal structure of the northeastern Taiwan area from seismic refraction data and its tectonic implication. *TAO*, **7**, 467-487.
- Cheng, W. B., C. Wang, and C. T. Shyu, 1996b: Crustal Velocity Structure and Seismic Wave Attenuation in Eastern-Southeastern Taiwan. *Proc. Sixth Taiwan Symposium on Geophysics*, 561-570.
- Cheng, W. B., C. Wang, and C. T. Shyu, 1997: Evidence for the existence of a remnant oceanic crust beneath the Coastal Range in eastern Taiwan. *Int. Conference and Sino-American Symposium on tectonics of East Asia*, 156.
- Chi, W. R., J. Namson, and J. Suppe, 1981: Stratigraphic record of plate interaction in the Coastal Range of eastern Taiwan. *Mem. Geol. Soc. China*, **4**, 155-194.
- Christensen, N. I., 1965: Compressional wave velocities in metamorphic rocks at pressures to 10 kbar. *J. Geophys. Res.*, **70**, 6147-6164.

- Christensen, N. I., 1979: Compressional wave velocities in rocks at high temperatures and pressures, critical thermal gradients, and crustal low velocity zones. *J. Geophys. Res.*, **84**, 6849-6857.
- Christensen, N. I., and W. D. Mooney, 1995: Seismic velocity structure and composition of the continental crust: a global view. *J. Geophys. Res.*, **100**, 9761-9788
- Eberhart-Phillips, D., 1986: Three-dimensional velocity structure in northern California Coast Ranges from inversion of local earthquakes arrival times. *Bull. Seism. Soc. Am.*, **76**, 1025-1052.
- Eberhart-Phillips, D., 1990: Three-dimensional P and S velocity structure in the Coalinga region, California. *J. Geophys. Res.*, **95**, 15343-15363.
- Eberhart-Phillips, D. and A. Michael, 1993: Three-dimensional velocity structure, seismicity, and fault structure in the Parkfield region, central California. *J. Geophys. Res.*, **98**, 15737-15758.
- Evans, J. R., D. Eberhart-Phillips, and C. H. Thurber, 1994: User's manual for SIMULPS 12 for imaging Vp and Vp/Vs: A derivative of the "Thurber" tomographic inversion SIMUL3 for local earthquake and explosions. U.S. Geol. Surv. Open File Rep., 94-431.
- Fuh, S. C., C. S. Liu, and G. S. Song, 1994: Decoupled transcurrent faults in the offshore area of Taiwan. *Pet. Geol. Taiwan*, **29**, 27-46.
- Fuh, S. C., C. S. Liu, N. Lundberg, and D. Reed, 1997: Strike-slip faults offshore southern Taiwan: implications for the oblique arc-continent collision processes. *Tectonophysics*, **274**, 25-39.
- Fuis, G. S., E. L. Ambos, W. Mooney, N. I. Christensen, and E. Geist, 1991: Crustal structure of accreted terranes in southern Alaska, Chugach Mountains and Copper River Basin, from seismic refraction results. *J. Geophys. Res.*, **96**, 4187-4227.
- Hauksson, E., and J. Hasse, 1997: Three-dimensional Vp and Vp/Vs velocity models of the Los Angeles basin and central transverse Range, California. *J. Geophys. Res.*, **102**, 5423-5453.
- Ho, C. S., 1982: Tectonic Evolution of Taiwan. Explanatory Text of the Tectonic Map of Taiwan. Minist. Econ. Affairs, Taipei, 126 pp.
- Ho, C. S., 1986: A synthesis of the geologic evolution of Taiwan. *Tectonophysics*, **125**, 1-16.
- Hsu, S. K., and J. C. Sibuet, 1995: Is Taiwan the result of arc-continent or arc-arc collision? *Earth Planet. Sci. Lett.*, **136**, 315-324.
- Huang, C. Y., C. T. Shyu, S. B. Lin, T. Q. Lee, and D. D. Sheu, 1992: Marine geology in the arc-continent collision zone off southeastern Taiwan: Implication for Late Neogene evolution of the Coastal Range. *Mar. Geol.*, **107**, 183-212.
- Huang, K. C., 1997: Earthquakes beneath southern Taiwan: a case of collision between Luzon arc and Taiwan. Master's Thesis, National Taiwan Univ. 160 pp. (in Chinese)
- Karig, D. E., 1973: Plate convergence between Philippines and the Ryukyu Islands. *Mar. Geol.*, **14**, 153-168.
- Kern, H., 1978: The effect of high temperature and high confining pressure on compressional wave velocities in quartz-bearing and quartz-free igneous and metamorphic rocks. *Tectonophysics*, **44**, 185-203.

- Kissling, E., W. L. Ellsworth, D. Eberhart-Phillips, and U. Kradolfer, 1994: Initial reference models in local earthquake tomography. *J. Geophys. Res.*, **99**, 19635-19646.
- Langston, C. A., 1981: Evidence for the subducting lithosphere under southern Vancouver Island and western Oregon from teleseismic P wave conversions. *J. Geophys. Res.*, **86**, 3857-3866.
- Lewis, S. D., and D. E. Hayes, 1989: Plate convergence and deformation, North Luzon Ridge, Philippines. *Tectonophysics*, **168**, 221-237.
- Lee, C. R., and W. T. Chang, 1986: Preliminary heat flow measurements in Taiwan. Circum-Pacific Energy and Mineral Resources Conf., 4th, Singapore.
- Lee, T. Q., J. Angelier, H. T. Chu, and F. Bergerat, 1991: Rotations in the northern eastern collision belt of Taiwan: preliminary results from paleomagnetism, *Tectonophysics*, **199**, 109-120.
- Lin, C. H., Y. H. Yeh, B. S. Huang, R. C. Shih, H. L. Lai, C. S. Huang, S. S. Yu, C. S. Yen, and F. T. Wu, 1997a: Deep crustal Structures inferred from wide-angle seismic data in Taiwan. Int. Conference and Sino-American Symposium on tectonics of East Asia, 155.
- Lin, C. H., Y. H. Yeh, H. Y. Yen, K. C. Chen, B. S. Huang, S. Roecker, and J. M. Chiu, 1997b: Three-dimensional elastic wave velocity structure of the Hualien region of Taiwan: evidence of active crustal exhumation. *Tectonics*, **17**, 89-103.
- Lin, M. T., and Y. B. Tsai, 1981: Seismotectonics in Taiwan-Luzon area. *Bull. Inst. Earth Sciences, Academia Sinica*, **1**, 51-82.
- Liu, S. Y., C. S. Liu, D. Reed, and N. Lundberg, 1992: Analysis of the tectonic structures in the region off southeastern Taiwan based on gravity-magnetic data. Proc. 4rd Taiwan Symposium on Geophysics, Taipei, Taiwan, 575-585.
- Liu, C. S., J. C. Su, and C. T. Shyu, 1991: Sedimentary structures of the arc-continent collision zone. Proc. 3rd Taiwan Symp. on Geophysics, Taipei, Taiwan, 458.
- Liu, C. S., 1995: Deep seismic imaging of the Taiwan arc-continent collision zone. Workshop for Integrated Oceanographic Research Programs, December 6-9, Taoyuan, T15-19.
- Ludwig, W. J., D. E. Hayes, and J. I. Ewing, 1967: The Manila Trench and West Luzon Trough, I. Bathymetry and sediment distribution. *Deep Sea Res.*, **14**, 533-544.
- Ludwig, W. J., S. Murauchi, N. Den, P. Puhl, H. Hotta, M. Ewing, T. Asanuma, T. Yoshii, and N. Sakajiri, 1973: Structure of East China Sea - West Philippine Sea margin off southern Kyushu, Japan. *J. Geophys. Res.*, **78**, 2526-2536.
- Lundberg, N., 1988: Present-day sediment transport paths south of the Longitudinal Valley, southeastern Taiwan. *Acta Geol. Taiwanica*, **26**, 317-331.
- Ma, K. F., J. H. Wang, and D. Zhao, 1996: 3-D seismic structure of the crust and uppermost mantle beneath Taiwan. *J. Phys. Earth*, **44**, 85-105.
- Menke, W., 1989: *Geophysical Data Analysis: Discrete Inverse Theory*. Academic, San Diego, Calif., 1-289.
- Michael, A., and D. Eberhart-Phillips, 1991: Relations among fault behavior, subsurface geology, and three-dimensional velocity models. *Science*, **253**, 651-654.
- Michellini, A., 1991: Fault zone structure determined through the analysis of earthquake ar-

- rival times. Ph. D. thesis, Univ. of Calif., Berkeley, 191pp.
- Michelini, A., and T. V. McEvilly, 1991: Seismological studies at Parkfield, I, Simultaneous inversion for velocity structure and hypocenters using cubic b-splines parameterization. *Bull. Seism. Soc. Am.*, **81**, 524-552.
- Mooney, W. D., 1989: Seismic methods for determining earthquakes source parameters and lithospheric structure. In: L. C. Pakiser and W. D. Mooney (Eds.), Geophysical Framework of the Continental United States, Geological Society of America Memoir, 172, 11-34.
- Mooney, W. D., G. Laske, and T. G. Masters, 1998: CRUST 5.1: A global crustal model at $5^{\circ} \times 5^{\circ}$. *J. Geophys. Res.*, **103**, 727-747.
- Page, B. M., and J. Suppe, 1981: The Pliocene Lichi Melange of Taiwan: its plate tectonic and olistostromal origin. *Am. Jour. Sci.*, **281**, 193-277.
- Pavlis, G. L., and J. R. Booker, 1980: The mixed discrete-continuous inverse problem: Application to the simultaneous determination of earthquake hypocenters and velocity structure. *J. Geophys. Res.*, **85**, 4801-4810.
- Pezzopane, S., and S. Wesnousky, 1989: Large earthquakes and crustal deformation near Taiwan. *J. Geophys. Res.*, **94**, 7250-7264.
- Rau, R. J., and F. T. Wu, 1995: Tomographic imaging of lithospheric structures under Taiwan. *Earth Planet. Sci. Lett.*, **133**, 517-532.
- Richard, M., H. Bellon, R.C. Maury, E. Barrier, and W. S. Juang, 1986: Miocene to recent calc-alkalic volcanism in eastern Taiwan: K-Ar ages and petrography. *Tectonophysics*, **125**, 87-102.
- Roecker, S. W., Y. H. Yeh, and Y. B. Tsai, 1987: Three-dimensional P and S wave velocity structures beneath Taiwan: deep structure beneath an arc-continent collision. *J. Geophys. Res.*, **92**, 10547-10570.
- Shyu, C. T., and S. C. Chen, 1991: A topographic and magnetic analysis off southeastern Taiwan. *Acta. Oceanogr. Taiwanica*, **27**, 1-20.
- Shyu, C. T., M. C. Chih, S. K. Hsu, C. Wang, and B. Karp, 1996: Northern Luzon arc: location and tectonic features from magnetic data off eastern Taiwan. *TAO*, **7**, 535-548.
- Sibuet, J. C., and S. K. Hsu, 1997: Geodynamics of the Taiwan arc-arc collision. *Tectonophysics*, **274**, 221-251.
- Spence, G. D., R. M. Clowes, and R. M. Ellis, 1985: Seismic structure across the active subduction zone of western Canada. *J. Geophys. Res.*, **90**, 6754-6772.
- Suppe, J., 1984: Kinematics of arc-continental collision, flipping of subduction, and back-arc spreading near Taiwan. *Mem. Geol. Soc. China*, **6**, 21-34.
- Toomey, D. R., and G. R. Foulger, 1989: Tomographic inversion of local earthquake data from the Hengill-Grensdalur central volcano complex, Iceland. *J. Geophys. Res.*, **94**, 17497-17510.
- Tsai, Y. B., T. L. Teng, J. M. Chiu, and H. L. Liu, 1977: Tectonic implications of the seismicity in the Taiwan region. *Mem. Geol. Soc. China*, **2**, 13-41.
- Thurber, C. H., 1983: Earthquake locations and three-dimensional crustal structure in the Coyote Lake area, central California. *J. Geophys. Res.*, **88**, 8226-8236.

- Thurber, C. H., 1993: Local earthquake tomography: Velocities and V_p/V_s – Theory, in Seismic Tomography. In: H. M. Iyer and Hirahara (Eds.), Theory and Practice, Chapman and Hall, New York, 563-583.
- Thurber, C., S. Roecker, W. Ellsworth, Y. Chen, W. Lutter, and R. Ressions, 1997: Two-dimensional seismic image of the San Andreas Fault in the Northern Gabilan Range, central California: evidence for fluids in the fault zone. *Geophys. Res. Lett.*, **24**, 1591-1594.
- Um, L., and C. H. Thurber, 1987: A fast algorithm for two-point seismic ray tracing. *Bull. Seism. Soc. Am.*, **77**, 972-986.
- Wu, F. T., 1978: Recent tectonics of Taiwan. *J. Phys. Earth*, **26**, S265-S299.
- Wu, F. T., and C. P. Lu, 1976: Recent tectonics of Taiwan. *Bull. Geol. Surv. Taiwan*, **25**, 97-111. (in Chinese)
- Yu, H. S., and G. S. Song, 1994: Oblique convergence between trench-arc system and continent: implication for the formation of the submarine physiography off southern Taiwan. *Acta. Oceanogr. Taiwanica*, **32**, 45-53.
- Yu, S. B., H. Y. Chen, and L. C. Kuo, 1997: Velocity field of GPS stations in the Taiwan area. *Tectonophysics*, **274**, 41-59.
- Zhao, D., A. Hasegawa, and S. Horiuchi, 1992: Tomographic imaging of P and S wave velocity structure beneath northeastern Japan. *J. Geophys. Res.*, **97**, 19909-19928